A. F. Ávila

aavila@netuno.lcc.ufmg.br
Universidade Federal de Minas Gerais
Department of Mechanical Engineering
31270-901 Belo Horizonte, MG, Brazil

L. G. Z. de O. Peixoto

Luisazica@yahoo.com.br
Universidade Federal de Minas Gerais
Graduate Program in Mechanical Engineering
31270-901 Belo Horizonte, MG, Brazil

A. Silva Neto

Almir.sneto@gmail.com
Universidade Federal de Minas Gerais
Graduate Program in Mechanical Engineering
31270-901 Belo Horizonte, MG, Brazil

J. de Ávila Junior

Jose.avila@javila.net
Universidade Federal de Minas Gerais
Graduate Program in Mechanical Engineering
31270-901 Belo Horizonte, MG, Brazil

M. G. R. Carvalho

Mariagabrielacarvalho@yahoo.com.br
Universidade Federal de Minas Gerais
Graduate Program in Mechanical Engineering
31270-901 Belo Horizonte, MG, Brazil

Bending Investigation on Carbon Fiber/Epoxy Composites Nano-Modified by Graphene

An extreme conditions situation, e.g. pre-salt deep sea exploration, requires new materials with even better performance. Nanotechnology is the new paradigm that can lead to the development of these new super materials. The effect of graphene pileups dispersion into carbon fiber/epoxy composites was investigated experimentally. The dispersion process was based on sonication and high shear mixing. XRD and SEM indicate that although the dispersion process can lead to exfoliated nanostructures, there is a saturation limit for the epoxy system, around 0.5 wt. %. The addition of graphene to carbon/epoxy composites seems to have no influence into stiffness, as the slopes of the stress-strain curves were near constant for all specimen tested. The bending strength, however, was heavily influenced by formation of graphene pileups into epoxy matrix and its dispersion around the carbon fibers. The increase on bending strength from 623.01±70.16 MPa (control samples) to 1259.92±61.73 MPa for 0.5 wt. % graphene addition represents an average improvement of 102%. This can be attributed to changes on failure mechanism, moving from intra-laminar failure to a mix failure mode where inter- and intra-laminar failure are combined in a zigzag pattern. A possible explanation for such behavior is the formation of strong bonds at the fiber/matrix surroundings due to nanostructures formation.
Keywords: *graphene, nanostructures, carbon/epoxy composites, bending properties, failure modes*

Introduction

According to Ávila et al. (2011), carbon based nano-structures, i.e. carbon nanotubes (CNT) and graphene nano sheets (GN), present remarkable mechanical, electrical and thermal properties. CNT capabilities have been observed experimentally and verified by numerical simulations. Although carbon nanotubes have great potential for applications in a large variety of usages, e.g. aerospace industry, medical and electronic devices, there is no consensus about their exact mechanical properties. Moreover, the high cost of CNT is an issue that cannot be discarded for industrial applications. Even though a large number of researchers have being using carbon nanotubes for reinforcement of composites laminates with good results. Among those researchers are Kim and collaborators (2009), whom described no significant increase on tensile properties of the addition of CNTs to carbon fibers/epoxy laminates. Nonetheless, they noticed an enhancement on flexural modulus (≈12%) and strength (≈18%) with the addition of 0.3 wt. % of CNT to the epoxy system. This increase can be attributed to changes into flexural failure mechanisms. Following the same idea, Chou et al. (2010) discussed the influence of CNTs into the failure of laminated composites. They even proposed the concept of a hybrid inter-laminar architecture that can bridge inter-laminar cracks. Wicks and colleagues (2010) actually produced the hybrid nano reinforced laminated composites proposed by Chou et al. (2010). As mentioned by Wicks, aligned CNTs bridge the plies interfaces, which can lead to an increase on toughness, for the steady state condition, 76%

higher than the conventional laminated systems. Notice that for the interlayer nano reinforcement some issues must be considered, i.e. the interfacial bonds between carbon nanotubes and the fiber/matrix system and the length effect into this "grip condition". Shokrieh and Rafiee (2010) modeled the CNT length effect on reinforcement effectiveness. Moreover, they concluded that for carbon nanotubes with length less than 100 nm, the improvement on stiffness for CNT/polymeric systems is negligible. By taking into consideration Shokrieh and Rafiee (2010) conclusions and the difficulties reported by Ma et al. (2010) for dispersing carbon nanotubes into polymeric matrices, it is clear that although CNTs are a viable option for reinforcement of nanocomposites and its hybrid companions, another alternative must be investigated.

Yasmin et al. (2007) mentioned that graphene based nanocomposites can be an alternative option for engineering applications due to their outstanding specific strength and stiffness. The usage of graphene nano sheets is gaining more attention due to their good relation benefit/cost. As said by Koo (2006), CNTs and graphene nano sheets (GN) have approximately the same stiffness, around 1.0 TPa. Moreover, the cost for expandable graphite, which is the main source of graphene nano sheets, is around US$10.00/pound, while single wall carbon nanotubes (CNT) cost for one single pound is 20,000 times higher.

To be able to apply graphene nano sheets to composite materials, the issue of polymer/nanoparticle compatibility must be investigated. Park and colleagues (2008) coated carbon fibers with exfoliated graphite by electro deposition to investigate its effect on mechanical properties. According to them, a small decrease on elongation around 11% was noticed when compared against conventional carbon fiber composites. However, an increase of

flexural modulus and strength was also observed. This increase was attributed to the reinforcement effect of the coated fibers. To be consistent with the coated fiber morphology, the increase on strength must be attributed to the interfacial bonds created by the coated fibers and the epoxy matrix. This could be the most likely explanation for the effect observed by Park et al. (2008). Park and co-workers did not discuss the possibility of breaking down the graphite nano sheets into graphene blocks. Drzal and his research group (Kalaitidou et al., 2007), however, introduced the idea of dispersing blocks of graphene into polymeric matrices. In their case, these matrices are thermoplastics, in special polypropylene (PP). By studying the graphene blocks dispersion into PP, Kalaitzidou et al. (2007) identified a saturation limit (around 10 wt. %) of graphene blocks for PP composites. After this limit, the flexural strength seems to reach a plateau. Li et al. (2007) went further, as they applied a surface treatment of graphite nano sheets based on ultraviolet light and ozone combination. Li and co-workers considered a nanocomposite based exclusively on epoxy and graphene based nanoparticles. They noticed a consistent increase on flexural modulus with the increase of graphene based nanoparticles up to 1.5 wt. %. Yet, a decrease on flexural strength was also identified with the increase of graphene content.

The purpose of this paper is to investigate the application of graphene nano sheets and clusters of graphene nano sheets into hybrid carbon fibers nanocomposites under bending loads.

Hybrid Nanocomposites Synthesis and Characterization

As commented by Ávila and co-workers (2010), the hybrid nanocomposites can be defined as multi-reinforced laminated composites. Such multi-reinforcement can be divided in three different levels; the first one is a nano-reinforcement with formation of nano-structures due to nanoparticles dispersion into the polymeric matrix. The second level of reinforcement can be described as the bond formed between clusters of nano-structures and the macroscopic fibers. Finally, fibers themselves can be defined as the last level of reinforcement.

In this research, the hybrid nanocomposite is a carbon fiber/nano-modified epoxy system laminated with 12 layers. The fiber reinforcement is a plain weave carbon fiber with a real density of 220 g/m^2. The epoxy system was made of diglycidil ether bisphenol A (DGBA) resin and an amine hardener, i.e. RemLam M and HY956, supplied by Huntsman Incorporated. The fiber/epoxy ratio is equal to 50/50. The graphene used has its origin from an expandable graphite (HC 11 IQ) supplied by Nacional Grafite Incorporated. When the HC 11 IQ expandable graphite is submitted to a 900^oC thermal gradient in a 30 second period or less, the polymeric layers between the graphite plies volatilize. This sudden reaction leads to the graphite speedy expansion. As the volume must remain constant, the graphite thickness approaches nano scale. The expanded graphite is later on functionalized using nitric and sulfuric acid solutions. The graphene nano sheets are obtained when the functionalized expanded graphite is sonicated in an aqueous solution for at least four hours, dried, and later on dispersed into epoxy matrix using a higher shear mix for at least one hour.

The hybrid composite was prepared following the procedure described by Ávila et al. (2010). A dispersant agent, acetone, was employed to improve the mixing process. A double mixing process was used during the samples preparations. The first step was sonication for one hour followed by higher shear mixing for another hour. The degassing stage was required to eliminate bubbles generated during the higher shear mixing, as well as to eliminate the dispersant agent, i.e. acetone. After this procedure, the hand lay-up with vacuum assisted cure was performed. As mentioned by Ávila and collaborators (2010b), the epoxy system has a saturation limit

for nanoparticles dispersion. After this limit, nanoparticles precipitation is most likely to occur. To be able to investigate the graphene effects, four different sets of specimens were prepared, i.e. 0 wt. %, 0.5 wt. %, 1.0 wt. % and 1.5 wt. %. Although the ASTM D 790 standard (2010) suggests 5 samples for each bending test, to be able to make a statistical analysis of data, 10 specimens were prepared for each case studied.

According to Koo and colleagues (2011), during the nanoparticles dispersion into polymeric matrices nano-structures are formed. The two most common detection techniques to nano-structures identification are X-ray diffraction and electronic microscopy. In this research, X-ray diffraction (XRD) experiments were carried out on a Shimadzu XRD-6000 X-ray diffract meter with Cu ($\lambda = 0.154$ nm) irradiation at 40 kV and 30 mA using a Ni filter. Data were recorded in the range from 2 to 80 deg in a continuous scanning at 2 degrees per minute and sampling pitch of 0.02 deg. The high resolution scanning electron microscope (HRSEM) used was a Quanta 200-FEG-FEI, while the transmission electron microscope (TEM) employed was a Tecnai – G2-20-FEI. During the three points bending tests, an EMIC DL10000 universal testing machine with load cell of 100 KN and electronic deflect meter of 25 mm was employed. The test procedure follows the ASTM D 790 standard (2010).

Data Analysis

Two different sets of experiments were performed. The first one deals with the nanostructures formed and its identification, while the second group of tests focuses on mechanical behavior and fracture analysis. HRSEM observations shown in Fig. 1(a) identify the expanded graphite structure before sonication. The expanded graphite seems to be formed of various thin layers of graphite grouped by van der Walls forces. However, these thin layers are also multi-layer materials. The tip of one of these layers is marked with the white circle in Fig. 1(a), while Fig. 1(b) is a TEM observation of a single layer of expandable graphite, showing the pileups of graphene nano sheets. Furthermore, Fig. 2 shows the X-ray diffraction (XRD) signature for control samples (0 wt. % graphene) and the three concentrations of graphene based hybrid nanocomposites, respectively.

As it can be noticed in Fig. 2, the sharp peaks occur between 26.21^o (0.0 wt. %) and 26.25^o (1.5 wt. %). The usage of Bragg's law (Cole, 1970) allows us to compute a basal spacing between 0.33 nm and 0.34 nm. According to Saito et al. (2005), the basal distance for pure graphene is around the 0.34 nm value. Furthermore, the XRD intensity seems to indicate a "saturation" limit as the highest peak was notice for the 0.5 wt. % samples. After the limit was reached the XRD intensity was decaying. The 1.5 wt. % samples presented XRD energy even lower than the control samples, i.e. 5193 CPS and 5597 CPS. This behavior could suggest the formation of clusters. This hypothesis was confirmed by high resolution SEM. Clusters of graphene nano sheets with 100 nm of diameter can be observed in Figs. 3(a)-(b). Finally, the "X-ray signature" seems to be an indication that the graphene nano sheets were exfoliated in blocks.

The next step was the mechanical characterization of these hybrid nanocomposites. Notice that the carbon/epoxy composites without graphene will be considered as control samples. This research focused on bending stiffness/strength due to the possible application of these composites as sandwich structures face sheets. Note that stresses are computed based on Timoshenko Beam Theory as described in Kollar and Springer (2003). By analyzing Fig. 4 some comments can be made. First, the graphene addition provided an increase on stiffness as it can be noticed in Tables 1 and 2. In all cases, the elasticity modulus in bending is statistically different, with the largest increase ($\approx$ 172%) for the 0.5 wt. % graphene samples. The large variation in modulus

can also be due to graphene agglomeration and cluster formation as seen in Fig. 3. Second, the strength was strongly affected by the graphene addition. A boost on peak stress of 139% was noticed for the 0.5 wt. % nanocomposite. As the amount of graphene increased, i.e. 1.0 wt. % and 1.5 wt. %, the peak stresses were 109% and 80% higher than the control samples (samples without graphene). This enhancement on peak stresses can be attributed to changes on failure modes. Statistical analyses, summarized in Tables 3 and 4, demonstrate that all four groups have a normal distribution and the Bonferroni test indicates, for $\alpha = 0.05$ (significance level), that there are significant statistical difference between the control sample group and the others. However, there is no difference among the groups with graphene.
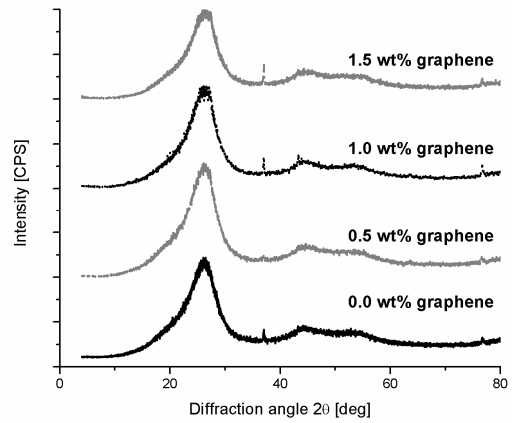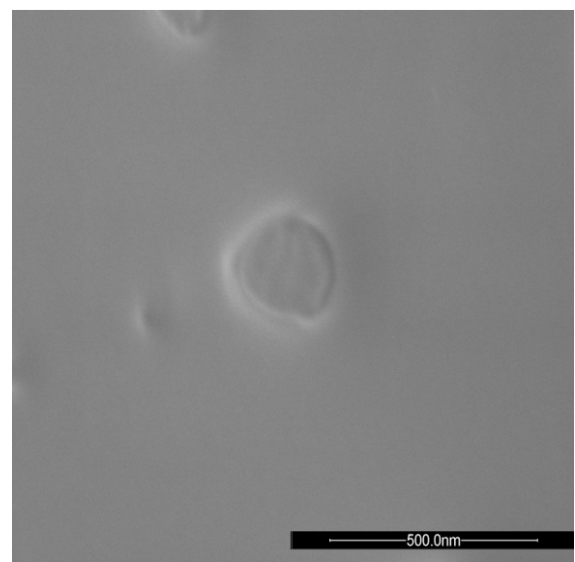

Figure 2. XRD signature.
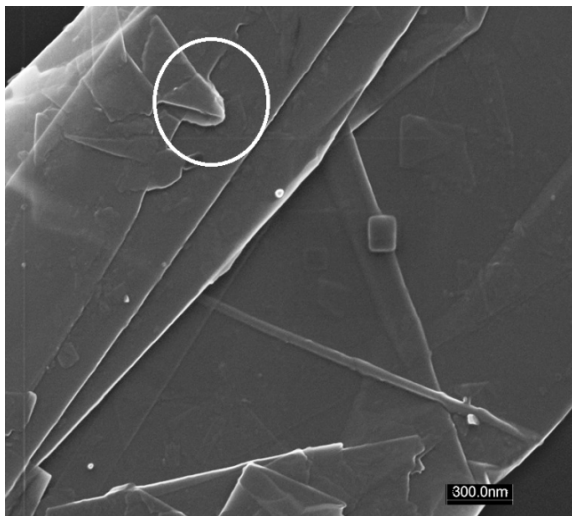
(a)
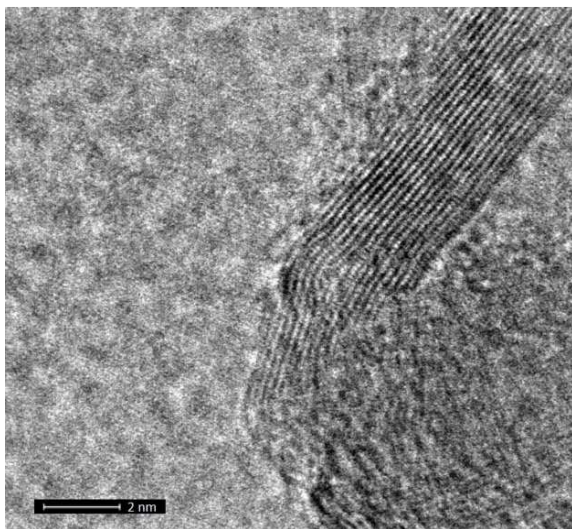
(b)

Figure 1. Single nanographite sheet observation: (a) SEM analysis; (b) TEM analysis.
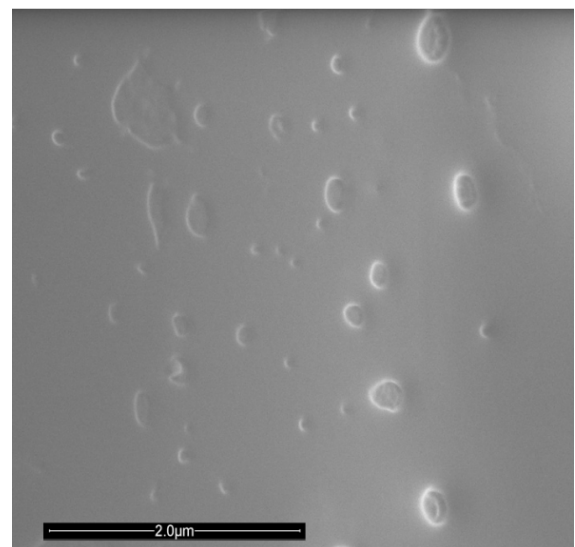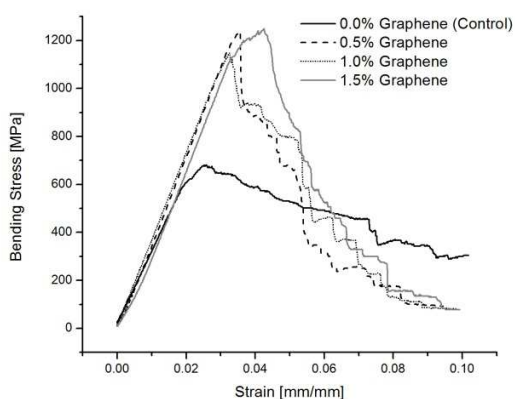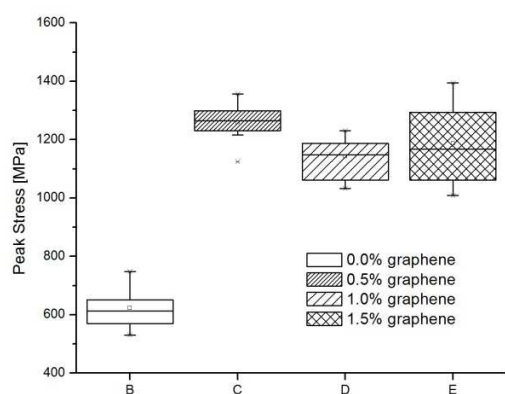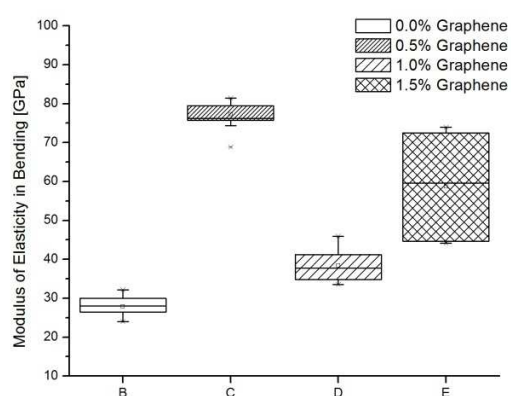

(a)

(b)

Figure 3. Graphene clusters: (a) Global view; (b) Zoom.

(a)

(b)

(c)

Figure 4. Stress-strain response to bending loads. (a) Typical Stress-strain curve; (b) Box graph for peak stresses; (c) Box graph for elasticity modulus in bending.

Table 1. Normality test – elasticity moduli in bending.

| Set ID	Mean Value [GPa]	Standard Deviation [GPa]	Mean Standard Error	Shapiro-Wilk*	
				W-statistical	p-value
0.0	27.9488	2.7373	0.9124	0.9537	0.7313
0.5	76.8675	4.0306	1.4250	0.8996	0.2869
1.0	38.4444	4.11937	1.3731	0.9388	0.5696
1.5	58.7142	13.2535	5.0093	0.8533	0.1319

*At the 0.05 level, the data was significantly draw from a normal distributed population.

Table 2. Bonferroni test – elasticity moduli in bending.

Groups	Mean Diff	Std. Error of Mean	t-value	p-value	Sig*
0.5-0.0	48.9186	3.3316	14.6828	3.4928E-14	1
1.0-0.0	10.4955	3.2322	3.2471	0.0176	1
1.0-0.5	-38.4230	3.4553	8.9036	5.1518E-9	1
1.5-0.0	30.7654	3.5485	-5.1156	1.1036E-4	1
1.5-0.5	-18.1532	3.4553	5.8661	1.3804E-5	1
1.5-1.0	20.2698	3.4553	8.9036	5.1518E-9	1

*Sig equals to 1 indicates that means difference is significant at the level 0.05. Sig equals to 0 indicates that means difference is not significant at the level 0.05.

Table 3. Normality test – peak stresses.

| Set ID	Mean Value [MPa]	Standard Deviation [MPa]	Mean Standard Error	Shapiro-Wilk*	
				W-statistical	p-value
0.0	623.0151	70.1557	23.3852	0.9492	0.6816
0.5	1259.919	61.7305	19.5209	0.9372	0.5228
1.0	1142.727	72.3982	22.8943	0.8958	0.1969
1.5	1187.536	129.549	40.9671	0.9478	0.6430

*At the 0.05 level, the data was significantly draw from a normal distributed population.

**Table 4. Bonferroni test – elasticity moduli in bending.**

Groups	Mean Diff	Std. Error of Mean	t-value	p-value	Sig*
0.5-0.0	636.9041	40.4967	15.7273	1.1601E-16	1
1.0-0.0	519.7120	40.4967	12.8334	5.1170E-14	1
1.0-0.5	-117.192	39.4166	-2.9731	0.0318	1
1.5-0.0	564.5215	40.4967	13.9399	4.4897E-15	1
1.5-0.5	-72.3825	39.4166	-1.8363	0.4488	0
1.5-1.0	44.8095	39.4166	1.1368	1	0

*Sig equals to 1 indicates that means difference is significant at the level 0.05. Sig equals to 0 indicates that means difference is not significant at the level 0.05.

According to Yasmin et al. (2007), bending failure on carbon fiber/epoxy systems is fiber dominated. Therefore, the failure propagation in all cases should be the same. However, when the test samples were analyzed, an unexpected behavior was noticed. The failure on control samples (Fig. 5(a)) was mainly intra-laminar, while the "zigzag" failure mode was observed in three sets of hybrid composites (Figs. 5(b)-5(d)). The zigzag failure mode can be described as a combination of inter- and intra-laminar failures. By allowing these two failure modes (inter- and intra-laminar) acting simultaneously the energy dissipation was improved, which leads to higher peak loads.
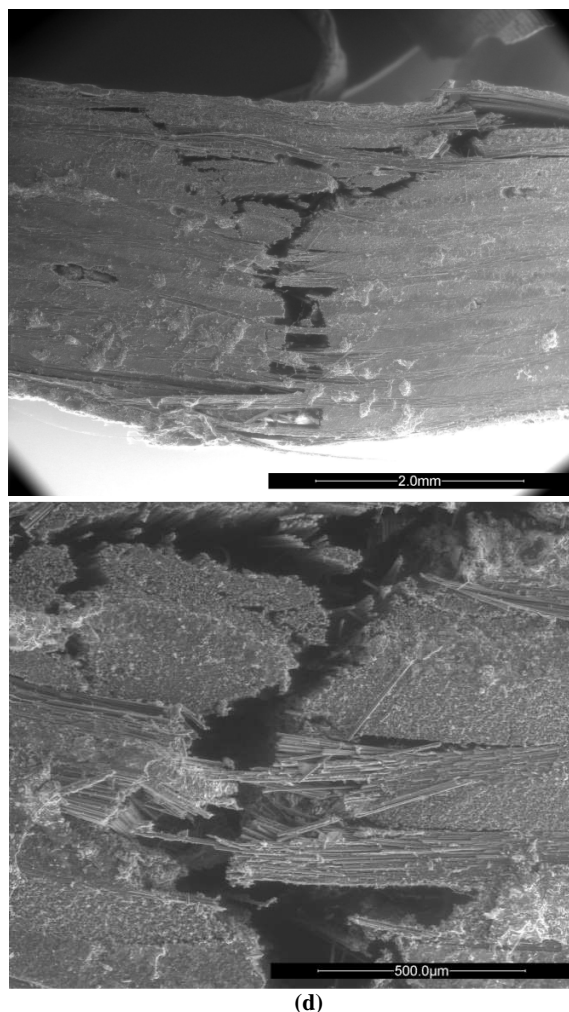
(a)

(b)

(c)

(d)
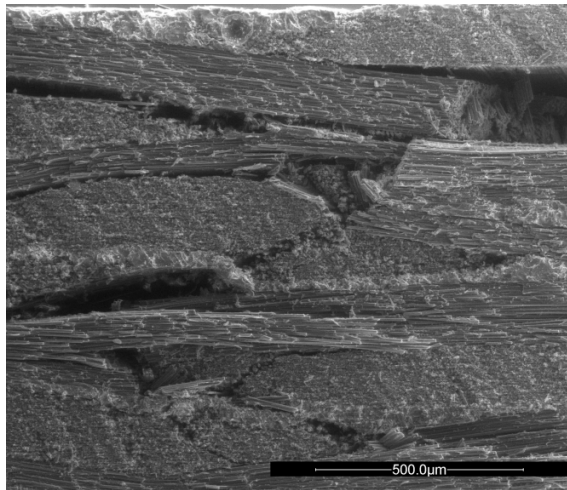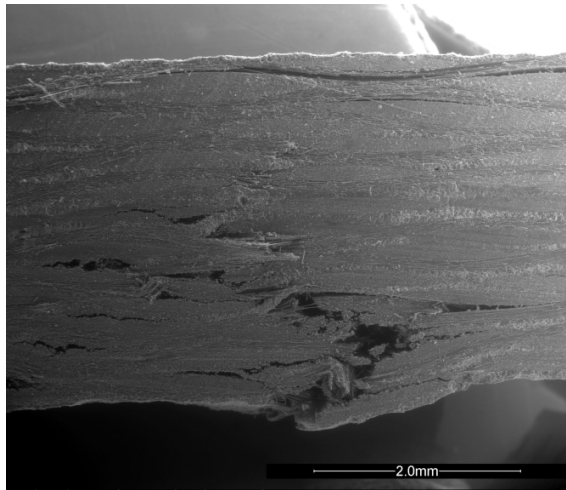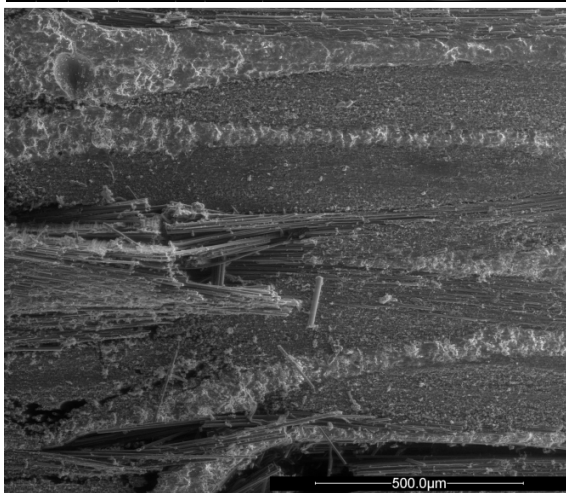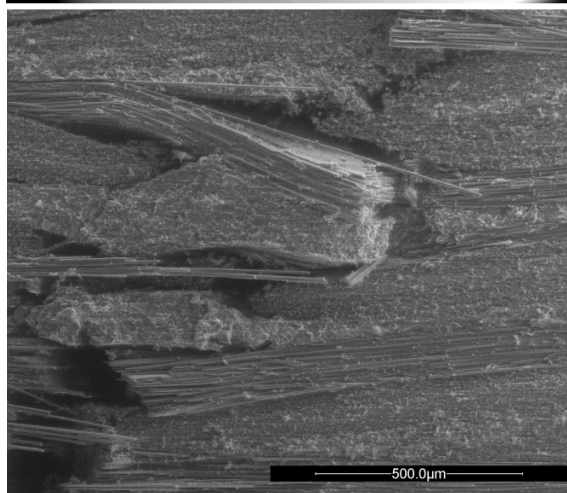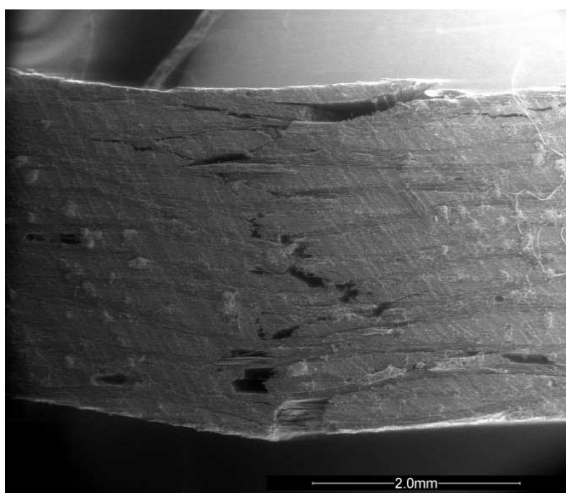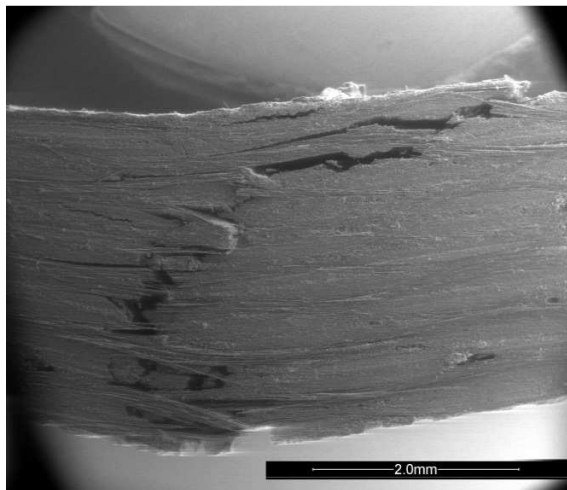
Figure 5. Failure modes versus graphene content. (a) 0wt. %; (b) 0.5wt. %; (c) 1.0wt. %; (d) 1.5wt. %.

A possible explanation for such behavior can be the graphene clusters dispersion into the matrix around the fibers, which can lead to formation of strong bonds at the interface fiber/matrix. These bonds could be responsible for stress distribution through the fibers and the zigzag effect. Notice that according to Kuilla and co-workers (2010), the graphene stiffness is around 1.0 TPa, and strength is close to 130 GPa, which can provide substantial increase on stiffness and strength of the interface fiber/matrix. This increase on strength and stiffness can provide a better stress distribution around the fiber/matrix surrounding region leading to a much higher bending strength. Notice that as the amount of dispersed graphene pileups increase, the epoxy matrix is approaching its saturation limit. After this limit, in our case 0.5 wt. %, precipitation occurs, which leads to clusters formation that will act as stress concentration sites. These clusters could be the cause of the decrease on bending strength with the increase of graphene dispersion from 0.5 wt. % to 1.0 wt. % and 1.5 wt. %, respectively. These clusters were spotted in specimens with 1.5 wt. %, as shown in Figs. 3(a) and 3(b).

Conclusions

The addition of graphene to carbon/epoxy laminated composites seems to influence into bending stiffness as well as on bending strength. The elasticity modulus in bending increased from 27.94 ± 2.74 GPa to 76.87 ± 4.03 GPa when the graphene addition went from 0 wt. % to 0.5 wt. %, respectively. A moderate increase on stiffness, 38.44 ± 4.12 GPa and 58.71 ± 13.25 GPa, was observed for the 1.0 wt. % and 1.5 wt. % samples. This small increase can be attributed to graphene clusters formation, due to the epoxy dispersion saturation limit. The bending strength was heavily influenced by the formation of graphene pileups into the epoxy matrix and its dispersion around the carbon fibers. The increase on bending strength reached a peak of 1355.94 MPa for the 0.5 wt. % specimens. As the amount of graphene dispersed into epoxy matrix increased, the average bending strength went from 623.01 ± 70.15 MPa (with no graphene) to 1259.91 ± 61.73 MPa (for a 0.5 wt. % graphene), and 1143.72 ± 72.39 MPa and 1187.53 ± 129.54 MPa, 1.0 wt. % and 1.5 wt. %, respectively. This enormous increase on bending strength can be attributed to changes on failure mechanism, moving from intra-laminar failure to a mix failure mode where inter- and intra-laminar failure are combined in a zigzag pattern. A possible explanation for such behavior is the formation of strong bonds at fiber/matrix surroundings due to nanostructures formation.

References

ASTM D 790, 2010, "Standard test methods for flexural properties of unreinforced and reinforced plastics and electrical insulating materials", Annual Book of ASTM Standards, Vol. 8, No. 1, pp. 104-112.

Ávila, A.F., Eduardo, A.C., Silva Neto, A., 2011, "Vibrational analysis of graphene based nanostructures", *Computers and Structures*, Vol. 89, No. 5, pp. 878-892.

Ávila, A.F., Yoshida, M.I., Carvalho, M.G.R., Dias, E.C., de Ávila Jr., J., 2010, "An investigation on post-fire behavior of hybrid nanocomposites under bending loads", *Composites Part B*, Vol. 41, No. 2, pp. 380-387.

Ávila, A.F., Carvalho, M.G.R., Dias, E.C., da Cruz, D.T., 2010b, "Nano-structured sandwich composites response to low velocity impact", *Composite Structures*, Vol. 92, No. 3, pp. 745-751.

Chou, T-W., Gao, L., Thostenson, E., Zhang, Z., Byun, J-H. 2010, "An assessment of the science and technology of carbon nanotube-based fibers and composites", *Composites Science and Technology*, Vol. 70, No. 1, pp. 1-19.

Cole, H., 1970, "Bragg's law and energy sensitive detector", *Journal of Applied Crystallography*, Vol. 3, No. 3, pp. 405-406.

Kalaitzidou, K., Fukushima, H., Drzal, L.T., 2007, "Mechanical properties and morphological characterization of exfoliated graphite–polypropylene nanocomposites", *Composites Part A*, Vol. 38, No. 8, pp. 1675-1682.

Kim, M., Park, Y-B., Okoli, O.I., Zhang, C. 2009, "Processing, characterization, and modeling of carbon nanotube-reinforced multiscale composites", *Composites Science and Technology*, Vol. 69, No. 2, pp. 335-342.

Kollar, L.P., Springer, G.S., 2003, "Mechanics of Composite Structures", Cambridge U.P., Cambridge, Chaps. 6,7.

Koo, J.H., 2006, "Polymer Nanocomposites: Processing, Characterization and Applications", McGraw-Hill, New York, Chaps. 3,7.

Koo, J.H., Loa, S.C., Lee, J., Chen, D.Z., Lam, C., Yong, W., Londa, M., Pilato, L.A., 2011, "Morphology and thermal characterization of nanographene platelets", *Journal of Materials Science*, Vol. 46, No. 10, pp. 3583-3589.

Kuilla, T., Bhadra, S., Yao, D., Kim, N.H., Bose, S., Lee, J.H., 2010, "Recent advances in graphene based polymer composites", *Progress in Polymer Science*, Vol. 35, No. 8, pp. 1350-1375.

Li, J., Sham, M. L., Kim, J-K, Marom, G., 2007, "Morphology and properties of UV/ozone treated graphite nanoplatelet/epoxy nanocomposites", *Composites Science and Technology*, Vol. 67, No. 2, pp. 296-305.

Ma, P-C., Siddiqui, N.A., Marom, G., Kim, J-K., 2010, "Dispersion and functionalization of carbon nanotubes for polymer-based nanocomposites: A review", *Composites Part A*, Vol. 41, No. 8, pp. 1345-1367.

Park, J.K., Do, I-H., Askeland, P., Drzal, L.T., 2008, "Electrodeposition of exfoliated graphite nanoplatelets onto carbon fibers and properties of their epoxy composites", *Composites Science and Technology*, Vol. 68, No. 6, pp. 1734-1741.

Saito, R., Dresselhaus, G., Dresselhaus, M.S. 2005, "Physical Properties of Carbon Nanotubes", 2nd ed., Imperial College Press, London, 2005, Chaps. 2,5.

Shokrieh, M.M., Rafiee, R., 2010, "Investigation of nanotube length effect on the reinforcement efficiency in carbon nanotube based composites", *Composite Structures*, Vol. 92, No. 10, pp. 2415-2420.

Yasmin, A., Luo, J-J., Daniel, I.M., 2006, "Processing of expanded graphite reinforced polymer nanocomposites", *Composites Science and Technology*, Vol. 66, No. 7, pp.1182-1189.

Wicks, S.S., de Villanova, R.G., Wardle, B.L., 2010, "Interlaminar and intralaminar reinforcement of composite laminates with aligned carbon nanotubes", *Composites Science and Technology*, Vol. 70, No. 1, pp. 20-28.